Journal of
Mechanics of
Materials and Structures

EFFECTS OF SURFACE AND INITIAL STRESSES ON THE BENDING STIFFNESS OF TRILAYER PLATES AND NANOFILMS

HanXing Zhu, JianXiang Wang and Bhushan Karihaloo

Volume 4, Nº 3 March 2009

mathematical sciences publishers

JOURNAL OF MECHANICS OF MATERIALS AND STRUCTURES
Vol. 4, No. 3, 2009

EFFECTS OF SURFACE AND INITIAL STRESSES ON THE BENDING STIFFNESS OF TRILAYER PLATES AND NANOFILMS

HANXING ZHU, JIANXIANG WANG AND BHUSHAN KARIHALOO

Simple closed-form analytic solutions have been obtained for the effect of initial residual stress on the bending stiffness of a symmetric trilayer plate/beam and for the combined effect of surface elasticity and initial surface stress on the bending stiffness of a nanofilm/nanobeam. The relative effect of the initial residual stress is generally limited to the range of the material yield strain. For nanofilms and nanobeams, the effect of the surface elasticity reduces with an increase in the thickness, but the initial surface stress effect can be retained at a constant level of up to the limit of elastic strain if it can be controlled, for example by the application of an electrical potential.

1. Introduction

Multilayer plate structures are widely used in applications at different size scales ranging from macro civil and mechanical structures down to microelectromechanical systems (MEMS) and nanoelectromechanical systems (NEMS). Elastic and thermal mismatch of individual materials can result in significant internal residual stresses in multilayer systems. As internal residual stresses can influence the overall mechanical properties (such as the stiffness and the natural frequency) and hence the dynamic and stability characteristics of multilayer systems, their determination has long interested material scientists and engineers [Stoney 1909; Freund 2000; Hui et al. 2000; Klein 2000; Dodin et al. 2001; Freund and Johnson 2001; Thompson and Clyne 2001; Donadon et al. 2002; Xu and Zhang 2003; Malzbender 2004; Huang and Zhang 2006; Huang and Zhang 2007]. Both the experimental measurement of internal stresses and the optimal design of multilayer systems rely heavily on the accuracy of the involved correlations. To the best of our knowledge, there is no reliable closed-form solution for the effect of initial residual stress on the bending stiffness of a symmetric trilayer plate structure (Figure 1).

The demand for smaller and faster devices has encouraged technological advances in the production of systems at micro- and nanoscales. While MEMS technology is now a well established area, nanoelectromechanical systems (NEMS) have been attracting more interest lately [Bunch et al. 2007; Masmanidis et al. 2007], as have the mechanical properties of nanomaterials and nanostructures. It has been well recognized that the effect of surface elasticity on the stiffness of nanostructures is size-dependent [He et al. 2004; Lim and He 2004; Cuenot et al. 2004; Zhou and Huang 2004; Duan et al. [2005a; 2005b; 2006]; Chen et al. 2006; Wang et al. 2006; Zhu and Karihaloo 2008]. As the surface to volume ratio is large, the stiffness and deformation of a nanostructure greatly depend on the surface stress, while the latter depends on the electric charge which in turn depends on the applied electric potential [Haiss et al. 1998; Weissmüller et al. 2003; Kramer et al. 2004]. Therefore the deformation of a nanostructure can be controlled by adjusting the applied electric potential [Kramer et al. 2004]. Miller and Shenoy [2000]

Keywords: residual stress, bending stiffness, surface effect, nanoplate, nanobeam.

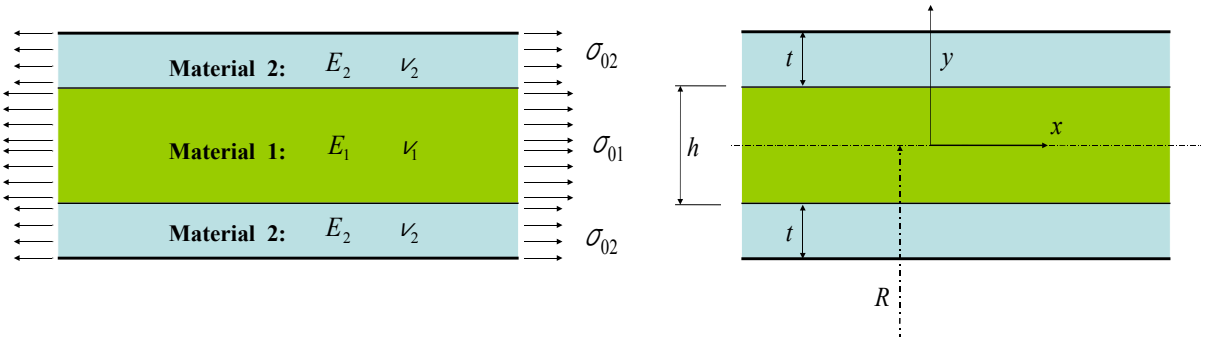

Figure 1. Schematic diagram of a prestressed trilayer plate. Left: materials and initial residual stresses. Right: dimensions and coordinate system.

showed that the relative contribution of the surface elastic modulus to the bending stiffness of a nanoplate is $6S/(Eh)$, where S is the surface elastic modulus, E is the Young's modulus of the bulk material and h is the thickness of the nanoplate.

However, the effect of the initial residual stresses on the bending stiffness of a nanoplate (or nanobeam) has not yet been considered. Zhu [2008] has considered the combined effects of surface elasticity and initial stresses on the bending stiffness of a core-shell nanowire with a circular cross-section. In this paper we consider the effect of initial stress on the bending stiffness of a symmetric trilayer plate/beam and the combined effects of surface elasticity and the initial stresses on the bending stiffness of a nanoplate/nanobeam with a rectangular or square cross-section.

2. Pure bending of a prestressed symmetric trilayer plate/beam

Figure 1 shows the cross-sectional geometry of a trilayer plate. The middle layer of thickness h is made of material 1 with Young's modulus E_1 and Poisson's ratio ν_1. Both the top and bottom layers of thickness t are made of material 2 with Young's modulus E_2 and Poisson's ratio ν_2. The width direction is denoted as z, which is normal to the xy-plane. The trilayer plate is initially flat and there is no initial residual stress in the thickness direction (that is, the y direction). The initial residual stresses in both the x and the z directions within the middle and the surface layers are σ_{01} and σ_{02}, respectively. Obviously, they satisfy the equilibrium condition

$$h\sigma_{01} + 2t\sigma_{02} = 0. \tag{1}$$

When the symmetric trilayer plate is bent by a pure moment M, the radius of the neutral surface is assumed to be R. To obtain a simple closed-form analytic solution for this problem, the following two assumptions are made: i) the materials are linear elastic and the deformation is very small; ii) the plate thickness does not change and R is much larger than the plate thickness. When a pure bending moment is applied to the initially flat symmetric trilayer plate, the deformed trilayer plate obviously becomes a cylinder but the initial cross-sectional planes remain plane after bending (as there is no net shear force in cross-sectional planes). As the superposition principle applies to this elastic small deformation problem, all the stresses and strains in the analysis of this paper, unless otherwise mentioned, are their changes from the initial prestressed state resulting from the application of the pure bending moment M.

When a wide trilayer plate is subjected to pure bending, the change of the strain in the z direction (which is normal to the xy-plane of Figure 1) ε_z is a constant through the thickness of the three layers and is to be determined. To simplify the analysis, we assume that thickness of the three layers does not change after bending and the neutral surface is always in the middle of the middle layer as the bending deformation is very small. This assumption will be subsequently validated.

We look at the deformation of the top layer first. Hooke's law requires

$$\sigma_2^z(y) = E_2\varepsilon_z + \nu_2\sigma_2^x(y) + \nu_2\sigma_2^y(y) \quad (h/2 \le y \le h/2+t), \tag{2}$$

where σ_2^z, σ_2^x, σ_2^y are the stress changes in the z, x and y directions, respectively and the subscript 2 refers to material 2 of the outer layers (Figure 1, left). All the stress changes are functions of the coordinate y (Figure 1, right). The equilibrium equation in the radial direction of the bent plate, namely $d\sigma^r/dr = (\sigma^\theta - \sigma^r)/r$, requires that

$$d(r\sigma_2^r) = \sigma_2^\theta dr,$$

where $\sigma_2^\theta = \sigma_2^x + \sigma_{02}$ and $\sigma_2^r = \sigma_2^y$. Integrating both sides and making use of the boundary condition $(r\sigma_2^r)|_{r=R+t+h/2} = 0$, we get for constant initial residual stress σ_{02} in the outer layers

$$\int_{R+y}^{R+t+h/2} d(r\sigma_2^r) = -(R+y)\sigma_2^y = \int_{R+y}^{R+t+h/2} \sigma_2^\theta dr = \int_y^{t+h/2} (\sigma_2^x + \sigma_{02})dy.$$

Since the thickness of the trilayer plate is far less than R (that is, $|y| \ll R$), this can be rewritten as

$$\sigma_2^y(y) = -\frac{1}{R+y}\int_y^{t+h/2} (\sigma_2^x + \sigma_{02})dy \approx -\frac{1}{R}\int_y^{t+h/2} (\sigma_2^x + \sigma_{02})dy. \tag{3}$$

Substituting (2) and (3) into Hooke's law

$$\varepsilon_2^x(y) = \frac{y}{R} = \frac{1}{E_2}(\sigma_2^x - \nu_2\sigma_2^z - \nu_2\sigma_2^y),$$

gives

$$\frac{yE_2}{R} = (1-\nu_2^2)\sigma_2^x(y) - \nu_2 E_2\varepsilon_z + \frac{\nu_2(1+\nu_2)}{R}\int_y^{t+h/2} \big(\sigma_2^x(y) + \sigma_{02}\big)dy. \tag{4}$$

Differentiating both sides with respect to y leads to

$$(1-\nu_2^2)\frac{d\sigma_2^x(y)}{dy} - \frac{\nu_2(1+\nu_2)}{R}\big(\sigma_2^x(y) + \sigma_{02}\big) - \frac{E_2}{R} = 0. \tag{5}$$

It should be mentioned that in (3), R is used to approximate r; otherwise, there is an additional term of $-\nu_2(1+\nu_2)r^{-2}\int_y^{t+h/2}\big(\sigma_2^x(y) + \sigma_{02}\big)dy$ on the left hand side of (5). As $1/r^2 \approx 1/R^2$ is a higher order small number, the term is ignored in the differential equation (5). The solution of the first order differential equation (5) is

$$\sigma_2^x(y) = A\exp\frac{\nu_2 y}{(1-\nu_2)R} - \frac{E_2}{\nu_2(1+\nu_2)} - \sigma_{02} \quad (h/2 \le y \le h/2+t), \tag{6}$$

where A is a constant of integration to be determined by substituting (6) into (4):

$$\begin{aligned} A &= \left(\frac{\nu_2 E_2 \varepsilon_z}{1-\nu_2^2} + \sigma_{02} + \frac{E_2}{\nu_2(1+\nu_2)} + \frac{(h+2t)E_2}{2R(1-\nu_2^2)}\right)\exp\left(-\frac{(h+2t)\nu_2}{2(1-\nu_2)R}\right) \\ &\approx \frac{\nu_2 E_2 \varepsilon_z}{1-\nu_2^2} - \frac{\nu_2^2 E_2 \varepsilon_z (h+2t)}{2(1-\nu_2)(1-\nu_2^2)R} + \sigma_{02} + \frac{E_2}{\nu_2(1+\nu_2)} - \frac{(h+2t)\nu_2\sigma_{02}}{2(1-\nu_2)R}. \end{aligned} \tag{7}$$

The exponential function has been expanded into a polynomial and the terms of order higher than $1/R$ have been ignored in (7), since $1/R$ is very small.

It is easy to see that (5) is also the governing differential equation for the stress change in the x direction within the bottom layer. The solution is therefore

$$\sigma_2^x(y) = B\exp\frac{\nu_2 y}{(1-\nu_2)R} - \frac{E_2}{\nu_2(1+\nu_2)} - \sigma_{02} \quad (-h/2 - t \le y \le -h/2), \tag{8}$$

where,

$$\begin{aligned} B &= \left(\frac{\nu_2 E_2 \varepsilon_z}{1-\nu_2^2} + \sigma_{02} + \frac{E_2}{\nu_2(1+\nu_2)} - \frac{(h+2t)E_2}{2R(1-\nu_2^2)}\right)\exp\left(\frac{(h+2t)\nu_2}{2(1-\nu_2)R}\right) \\ &\approx \sigma_{02} + \frac{E_2}{\nu_2(1+\nu_2)} + \frac{(h+2t)\nu_2\sigma_{02}}{2(1-\nu_2)R} + \frac{\nu_2 E_2 \varepsilon_z}{1-\nu_2^2} + \frac{\nu_2^2 E_2 \varepsilon_z (h+2t)}{2(1-\nu_2)(1-\nu_2^2)R}. \end{aligned} \tag{9}$$

In a similar manner, the governing differential equation for the stress change in the x direction within the middle layer can be obtained as

$$(1-\nu_1^2)\frac{d\sigma_1^x(y)}{dy} - \frac{\nu_1(1+\nu_1)}{R}\left(\sigma_1^x(y) + \sigma_{01}\right) - \frac{E_1}{R} = 0 \quad (-h/2 \le y \le h/2), \tag{10}$$

where the subscript 1 refers to material 1 of the middle layer. The solution of (10) is

$$\sigma_1^x(y) = C\exp\frac{\nu_1 y}{(1-\nu_1)R} - \frac{E_1}{\nu_1(1+\nu_1)} - \sigma_{01} \quad (-h/2 \le y \le h/2), \tag{11}$$

where the constant of integration is given by

$$C = \left(\frac{\nu_1 E_1 \varepsilon_z}{1-\nu_1^2} + \sigma_{01} + \frac{E_1}{\nu_1(1+\nu_1)} - \frac{t\nu_1}{(1-\nu_1)R}A + \frac{tE_2\nu_1}{\nu_2(1+\nu_2)(1-\nu_1)R} + \frac{hE_1}{2(1-\nu_1^2)R}\right)\exp\left(-\frac{\nu_1 h}{2(1-\nu_1)R}\right)$$

for $0 \le y \le h/2$ and by

$$C = \left(\frac{\nu_1 E_1 \varepsilon_z}{1-\nu_1^2} + \sigma_{01} + \frac{E_1}{\nu_1(1+\nu_1)} + \frac{t\nu_1}{(1-\nu_1)R}B - \frac{tE_2\nu_1}{\nu_2(1+\nu_2)(1-\nu_1)R} - \frac{hE_1}{2(1-\nu_1^2)R}\right)\exp\left(-\frac{\nu_1 h}{2(1-\nu_1)R}\right)$$

for $-h/2 \le y \le 0$; in either case, we have

$$C \approx \frac{\nu_1 E_1 \varepsilon_z}{1-\nu_1^2} + \frac{\nu_1^2 E_1 \varepsilon_z h}{2(1-\nu_1)(1-\nu_1^2)R} + \sigma_{01} + \frac{E_1}{\nu_1(1+\nu_1)} \quad (-h/2 \le y \le h/2).$$

(Here we have used (1), (7), (9) and the relationships $\sigma_1^z(y) = E_1\varepsilon_z + \nu_1\sigma_1^x(y) + \nu_1\sigma_1^y(y)$ (valid for $-h/2 \le y \le h/2$) and $\varepsilon_1^x(y) = y/R = (1/E_1)(\sigma_1^x - \nu_1\sigma_1^z - \nu_1\sigma_1^y)$.)

Therefore, the change of the stress in the x direction within the symmetric trilayer plate after the application of the external pure bending moment M is

$$\sigma^x(y) = \begin{cases} A\exp\dfrac{\nu_2 y}{(1-\nu_2)R} - \dfrac{E_2}{\nu_2(1+\nu_2)} - \sigma_{02} & (h/2 \le y \le t+h/2), \\ C\exp\dfrac{\nu_1 y}{(1-\nu_1)R} - \dfrac{E_1}{\nu_1(1+\nu_1)} - \sigma_{01} & (-h/2 \le y \le h/2), \\ B\exp\dfrac{\nu_2 y}{(1-\nu_2)R} - \dfrac{E_2}{\nu_2(1+\nu_2)} - \sigma_{02} & (-t-h/2 \le y \le -h/2), \end{cases} \tag{12}$$

which can be rewritten as

$$\sigma^x(y) = \frac{\nu_2 E_2 \varepsilon_z}{1-\nu_2^2} - \frac{\nu_2^2 E_2 \varepsilon_z (h+2t)}{2(1-\nu_2)(1-\nu_2^2)R} + \frac{\nu_2^2 E_2 \varepsilon_z y}{(1-\nu_2)(1-\nu_2^2)R} - \frac{\nu_2 \sigma_{02}}{(1-\nu_2)R}\left(\frac{h}{2}+t-y\right) + \frac{E_2 y}{(1-\nu_2^2)R}$$

for $h/2 \le y \le t+h/2$,

$$\sigma^x(y) = \frac{\nu_1 E_1 \varepsilon_z}{1-\nu_1^2} + \frac{\nu_1^2 E_1 \varepsilon_z h}{2(1-\nu_1)(1-\nu_1^2)R} + \frac{\nu_1^2 E_1 \varepsilon_z y}{(1-\nu_1)(1-\nu_1^2)R} + \frac{\nu_1 \sigma_{01}}{(1-\nu_1)R} y + \frac{E_1 y}{(1-\nu_1^2)R}$$

for $-h/2 \le y \le h/2$, and

$$\sigma^x(y) = \frac{\nu_2 E_2 \varepsilon_z}{1-\nu_2^2} + \frac{\nu_2^2 E_2 \varepsilon_z (h+2t)}{2(1-\nu_2)(1-\nu_2^2)R} + \frac{\nu_2^2 E_2 \varepsilon_z y}{(1-\nu_2)(1-\nu_2^2)R} + \frac{\nu_2 \sigma_{02}}{(1-\nu_2)R}\left(\frac{h}{2}+t+y\right) + \frac{E_2 y}{(1-\nu_2^2)R}$$

for $-t-h/2 \le y \le -h/2$.

Now we look at the amplitude of the strain change in the z direction ε_z. The cylindrical bending condition requires a zero resultant force in the z direction

$$F_z = \int_{R-t-h/2}^{R+t+h/2} r\sigma^z dr = 0. \tag{13}$$

Substituting (2), (12) and $\sigma_1^z(y) = E_1\varepsilon_z + \nu_1\sigma_1^x(y) + \nu_1\sigma_1^y(y)$ into (13), one has

$$\begin{aligned} F_z &= \int_{R-t-h/2}^{R+t+h/2} r\sigma^z dr \\ &= 2tE_2\varepsilon_z R + hE_1\varepsilon_z R + \nu_2 \int_{R-t-h/2}^{R+t+h/2} (\sigma^x + \sigma^y) r\,dr + (\nu_1 - \nu_2) \int_{R-h/2}^{R+h/2} (\sigma_1^x + \sigma_1^y) r\,dr. \end{aligned} \tag{14}$$

Here $r = R + y$. It is easy to verify that

$$\nu_2 \int_{R-t-h/2}^{R+t+h/2} (\sigma^x + \sigma^y) r\,dr = \nu_2 r^2 \sigma^y \Big|_{y=-t-h/2}^{y=t+h/t} = 0, \tag{15}$$

as there is no traction on the outside surface of the top and the bottom layers, and

$$(\nu_1 - \nu_2) \int_{R-h/2}^{R+h/2} (\sigma_1^x + \sigma_1^y) r\,dr = \frac{\nu_1 - \nu_2}{2} r^2 \sigma^y \Big|_{y=-h/2}^{y=h/2}. \tag{16}$$

Substituting (14)–(16) into (13) and ignoring the terms of order higher than $1/R$, one has

$$\varepsilon_z = \frac{\dfrac{\nu_2(\nu_1-\nu_2)(1+2t/h)}{1-\nu_2}\dfrac{\sigma_{02}t}{E_2R}}{8t/h+\dfrac{4E_1}{E_2}-\dfrac{2\nu_2(1-\nu_2)t}{(1-\nu_2^2)R}+\dfrac{2(\nu_1-\nu_2)\nu_2^2(1+2t/h)t}{(1-\nu_2)(1-\nu_2^2)R}} \approx \frac{\nu_2(\nu_1-\nu_2)(1+2t/h)}{(8t/h+4E_1/E_2)(1-\nu_2)^2}\cdot\frac{t}{R}\varepsilon_{02}, \quad (17)$$

where $\varepsilon_{02}=\sigma_{02}(1-\nu_2)/E_2$ is the initial elastic residual strain in the top or bottom layer before the application of the bending moment M. Equation (17) shows clearly that ε_z is zero if $\nu_1=\nu_2$. As t/R is very small, $|\varepsilon_z| \ll |\varepsilon_{02}|$ when $\nu_1 \neq \nu_2$, it will be set equal to zero to simplify the analysis that follows.

The total stress in the x direction within the symmetric trilayer plate after the application of the external pure bending moment M is given by superposition

$$\Sigma^x(y) = \sigma^x(y) + \begin{cases}\sigma_{02}\\ \sigma_{01}\\ \sigma_{02}\end{cases}$$

$$= \begin{cases} \sigma_{02} - \dfrac{\nu_2\sigma_{02}}{(1-\nu_2)R}\left(\dfrac{h}{2}+t-y\right)+\dfrac{E_2y}{(1-\nu_2^2)R} & (h/2\le y\le t+h/2),\\ \sigma_{01}+\dfrac{\nu_1\sigma_{01}}{(1-\nu_1)R}y+\dfrac{E_1y}{(1-\nu_1^2)R} & (-h/2\le y\le h/2),\\ \sigma_{02}+\dfrac{\nu_2\sigma_{02}}{(1-\nu_2)R}\left(\dfrac{h}{2}+t+y\right)+\dfrac{E_2y}{(1-\nu_2^2)R} & (-t-h/2\le y\le -h/2). \end{cases} \quad (18)$$

It is easy to verify the following facts:

- There is no net resultant axial force in the trilayer plate in the x direction: $N_x=\displaystyle\int_{-t-h/2}^{t+h/2}\Sigma^x(y)\,dy=0$.
- The stress in the radial direction (the y direction in Figure 1), given by

$$\sigma^y(y) = -\frac{1}{R}\int_y^{t+h/2}\Sigma^x(y)\,dy$$

  (the equilibrium condition in the y direction), satisfies the stress continuity condition across the neutral surface and the interfaces between the middle and the surface layers.
- There is no traction in the y direction on both the top and bottom surfaces; that is, $\sigma_2^y(t+h/2)=\sigma_2^y(-t-h/2)=0$.

For a given bending curvature $1/R$, we are now in a position to compute the amplitude of the applied bending moment

$$M=\int_{-t-h/2}^{t+h/2}\Sigma^x(y)\,y\,dy. \quad (19)$$

Substituting (18) into (19), the bending stiffness of the prestressed symmetric trilayer plate can be obtained as

$$D=M/(1/R)=\frac{E_2\left((h+2t)^3-h^3\right)}{12(1-\nu_2^2)}+\frac{E_1h^3}{12(1-\nu_1^2)}+\frac{\nu_1\sigma_{01}h^3}{12(1-\nu_1)}-\frac{\nu_2\sigma_{02}t^2(3h+2t)}{6(1-\nu_2)}. \quad (20)$$

When the initial residual stresses σ_{02} and σ_{01} are absent, the bending stiffness of the symmetric trilayer plate is denoted by

$$D_0 = \frac{E_2\big((h+2t)^3 - h^3\big)}{12(1-\nu_2^2)} + \frac{E_1 h^3}{12(1-\nu_1^2)}. \tag{21}$$

From equations (20) and (21), the contribution of the initial residual stresses to the bending stiffness of a symmetric trilayer plate is therefore

$$\begin{aligned} D - D_0 &= \frac{\sigma_{01}}{12}\left(\frac{\nu_1 h^3}{1-\nu_1} + \frac{\nu_2 t h(3h+2t)}{1-\nu_2}\right) = \frac{E_1\varepsilon_{01}}{12(1-\nu_1)}\left(\frac{\nu_1 h^3}{1-\nu_1} + \frac{\nu_2 t h(3h+2t)}{1-\nu_2}\right) \\ &= -\frac{\sigma_{02}}{6}\left(\frac{\nu_1 t h^2}{1-\nu_1} + \frac{\nu_2 t^2(3h+2t)}{1-\nu_2}\right) = -\frac{E_2\varepsilon_{02}}{6(1-\nu_2)}\left(\frac{\nu_1 t h^2}{1-\nu_1} + \frac{\nu_2 t^2(3h+2t)}{1-\nu_2}\right). \end{aligned} \tag{22}$$

Equation (1) has been used in obtaining (22), where $\varepsilon_{01} = (1-\nu_1)\sigma_{01}/E_1$ and $\varepsilon_{02} = (1-\nu_2)\sigma_{02}/E_2$ are the initial residual strains within the middle and extreme layers. Equation (22) shows clearly that an initial tensile residual stress or strain (that is, $\varepsilon_{01} > 0$) in the middle layer increases the bending stiffness of a trilayer plate. If the plate is made of a metallic material, the initial effective residual stresses should be smaller than the yield strength of the metal. According to the von Mises yield criterion, one has

$$|\varepsilon_{01}| = (1-\nu_1)|\sigma_{01}|/E_1 \le (1-\nu_1)\sigma_{y1}/E_1 = (1-\nu_1)\varepsilon_{y1} \tag{23a}$$

and likewise

$$|\varepsilon_{02}| \le (1-\nu_1)\varepsilon_{y2}. \tag{23b}$$

Equations (22) and (18) can be used to optimize the design and to determine experimentally the residual stresses or material properties for symmetric trilayer structures such as thermal barrier coated engine blades. Equations (23a) and (23b) give the limits for the possible amplitude of the initial residual elastic strains in symmetric trilayer structures. However, if a trilayer structure is made of a hyper-elastic material, such as a polymer or a rubber, the initial linear elastic residual strain could be as large as a few percent.

Now we consider the pure bending of a symmetric trilayer beam with a rectangular cross-section. The structure, the coordinate system, the initial residual stresses and strains of the unbent symmetric trilayer beam are the same as those of the unbent symmetric trilayer plate. The only difference is its width dimension in the z direction of Figure 1. When it is bent by a pure moment, the deformation is assumed to satisfy the plane stress condition. Following the above analysis procedure, it can be shown that the total stresses in the x direction within the trilayer beam are

$$\Sigma^x(y) = \begin{cases} \sigma_{02} - \dfrac{\nu_2\sigma_{02}}{R}\left(\dfrac{h}{2} + t - y\right) + \dfrac{E_2 y}{R} & (h/2 \le y \le t + h/2), \\ \sigma_{01} + \dfrac{\nu_1\sigma_{01}}{R} y + \dfrac{E_1 y}{R} & (-h/2 \le y \le h/2), \\ \sigma_{02} + \dfrac{\nu_2\sigma_{02}}{R}\left(\dfrac{h}{2} + t + y\right) + \dfrac{E_2 y}{R} & (-t - h/2 \le y \le -h/2). \end{cases} \tag{24}$$

The bending stiffness of the prestressed beam is therefore

$$D = \frac{E_2\big((h+2t)^3 - h^3\big)}{12} + \frac{E_1 h^3}{12} + \frac{\nu_1\sigma_{01}h^3}{12} - \frac{\nu_2\sigma_{02}t^2(3h+2t)}{6}. \tag{25}$$

When the initial residual stresses σ_{02} and σ_{01} are absent, the bending stiffness of the symmetric trilayer beam is denoted as

$$D_0 = \frac{E_2\big((h+2t)^3 - h^3\big)}{12} + \frac{E_1 h^3}{12}. \tag{26}$$

The effect of the initial residual stresses on the bending stiffness is

$$D - D_0 = \frac{\nu_1 \sigma_{01} h^3}{12} - \frac{\nu_2 \sigma_{02} t^2 (3h+2t)}{6}. \tag{27}$$

Obviously, the relative effect of the initial residual stresses on the bending stiffness of a symmetric trilayer beam is at the same level as on that of a symmetric trilayer plate discussed above.

Following the line of the analysis in this paper or in [Zhu 2007], it is possible to obtain the exact closed-form analytical solution for large curvature elastic pure bending of the same structure. However, as the exact solution is a very lengthy function, it is not convenient to use in practice. Although it is easy to obtain a numerical solution for large curvature elastic bending, it is difficult to see the correlations between the different parameters such as the structure dimensions, the material properties and the initial residual stresses (or strains). That is why we have simplified the analysis above to obtain a simple closed-form solution for small curvature.

The simplified closed-form solution is valid not only for macro civil structures, but also for micro- and nanostructures. The schematic symmetric trilayer structure shown in Figure 1 is one of the most typical structures of microactuators. For example, a typical conducting polymeric actuator consists of a polymer membrane (usually, Nafion, Flemion or Aciplex) covered on both faces by a noble metal, generally platinum or gold [Nemat-Nasser 2002; Alici et al. 2005]. When the actuator is stimulated by the application of a small (1–3 V) alternating potential, it undergoes flexural vibrations [Nemat-Nasser 2002]. The precision, resolution and reliability of such a MEMS system mainly depend on its mechanical structure. The outcome of this paper provides an enhanced degree of understanding and predictability in quantifying the actuator's performance and hence paves the way towards the optimal design and precise experimental measurement of such structures.

3. Pure bending of a nanoplate/nanobeam

For nanostructures, as the surface to volume ratio is large, the surface elasticity, in addition to any residual surface stresses, plays a very important role in the deformation process [Cuenot et al. 2004; Duan et al. 2005a; 2005b; 2006; Chen et al. 2006; Wang et al. 2006; Zhu and Karihaloo 2008]. In continuum models, nanoplates are usually treated as "sandwich structures" consisting of the bulk material and very thin facets [He et al. 2004; Lim and He 2004; Miller and Shenoy 2000; Lu et al. 2006]. The linear constitutive relation of the surface can be written as [Miller and Shenoy 2000; Cammarata and Sieradzki 1994]

$$\tau_{ij} = \tau_{ij}^0 + S_{ijkl}\varepsilon_{kl}, \tag{28}$$

where τ_{ij} is the surface stress after deformation , τ_{ij}^0 is the initial stress before deformation, S_{ijkl} is the surface modulus tensor and ε_{kl} is the surface strain. The surface stress and surface elastic constants have reduced dimensionality. It has been found that the effect of surface elastic modulus on the stiffness of nanostructures is size-dependent. The effect of surface elasticity on the mechanical properties of materials and structures has been extensively studied [Miller and Shenoy 2000; Lu et al. 2006; Gurtin

and Murdoch 1975], and the relative contribution of the surface elasticity to the bending stiffness of a nanoplate has been found to be $6S/(Eh)$, where S is the surface elastic modulus, E is the Young's modulus of the bulk material and h is the thickness of the nanoplate [Miller and Shenoy 2000]. This contribution does not include the effect of any initial surface stress.

For a nanoplate, the surfaces are notionally assumed so only in a mathematical sense, whose thickness t is much smaller than the thickness h of the core of the plate. In this case, we still use Figure 1 as the structural model and the stresses are assumed not to change through thickness of the top and the bottom surfaces. Similarly to the macroplate, we assume that when the nanoplate is bent to a very small curvature $1/R$ (R is much larger the plate thickness h) by a pure bending moment, both the "surface" and the bulk material are linear elastic; and the thickness of the nanoplate remains unchanged. Obviously the original cross-sectional planes remain plane as there is no net shear force in the cross-sectional planes. It is easy to verify that the neutral surface is still in the middle of the bulk plate. Therefore, the stresses in the x direction in the top and bottom surfaces are respectively

$$\tau_t^x = \tau_0 + \frac{S}{1-\nu_2^2}\frac{h}{2R} \ \text{(N/m)} \quad \text{and} \quad \tau_b^x = \tau_0 - \frac{S}{1-\nu_2^2}\frac{h}{2R} \ \text{(N/m)}, \tag{29}$$

where τ_0 is the initial surface stress, S is the surface elastic modulus and ν_2 is the Poisson ratio of the surfaces.

The stresses in the y direction on the top and bottom interfaces of bent bulk plate are respectively

$$\sigma_1^y\big|_{y=h/2} = -\frac{\tau_t^x}{R} \approx -\frac{\tau_0}{R} \quad \text{and} \quad \sigma_1^y\big|_{y=-h/2} = \frac{\tau_b^x}{R} \approx \frac{\tau_0}{R}. \tag{30}$$

In the similar manner, it is easy to verify that (10) is still the governing differential equation for the stress change in the x direction within the bulk plate. The solution to the stress change in the x direction within the bulk plate is the same as (11), but the constant of integration C is determined by making use of the stress continuity conditions (30) in the radial direction across the top and bottom interfaces,

$$C = \sigma_{01} + \frac{E_1}{\nu_1(1+\nu_1)} \quad (-h/2 < y < h/2). \tag{31}$$

As before, the exponential function has been replaced by a polynomial function with the terms of order higher than $1/R$ ignored, and the equilibrium condition $\sigma_{01} = -\frac{2\tau_0}{h}$ has been used in deriving the solution. Therefore the total stress in the x direction within the bulk plate after the application of the external pure bending moment M is given by superposition

$$\Sigma^x(y) = -\frac{2\tau_0}{h} - \frac{2\nu_1\tau_0}{(1-\nu_1)h}\frac{y}{R} + \frac{E_1 y}{(1-\nu_1^2)R} \quad (-h/2 < y < h/2). \tag{32}$$

On the top and the bottom surfaces, the surface stresses are given in (29).

The applied pure bending moment can be calculated as

$$M = \frac{Sh^2}{2(1-\nu_2^2)R} + \int_{-h/2}^{h/2} \Sigma^x(y)\, y\, dy$$

and the bending stiffness of a nanoplate is therefore

$$D = \frac{Sh^2}{2(1-\nu_2^2)} + \frac{E_1 h^3}{12(1-\nu_1^2)} - \frac{\nu_1 \tau_0 h^2}{6(1-\nu_1)}. \tag{33}$$

Since $D_0 = \frac{1}{12} E_1 h^3/(1-\nu_1^2)$ is conventionally taken as the bending stiffness of a nanoplate when the surface effect is absent, the relative contribution of the initial residual surface stress τ_0 and the surface elasticity to the elastic bending capacity is therefore

$$\frac{D-D_0}{D_0} = \frac{6S(1-\nu_1^2)}{(1-\nu_2^2)E_1 h} - \frac{2\tau_0 \nu_1 (1+\nu_1)}{E_1 h} = \frac{6(1-\nu_1^2)}{(1-\nu_2^2)} \cdot \frac{\ell_n}{h} + \frac{\nu_1(1+\nu_1)}{1-\nu_1}\varepsilon_{01}, \tag{34}$$

where

$$\varepsilon_{01} = \frac{(1-\nu_1)\sigma_{01}}{E_1} = -\frac{2(1-\nu_1)\tau_0}{E_1 h}$$

is the initial elastic residual strain within the core of the nanoplate and $\ell_n = S/E_1$ is an intrinsic length scale. Since the plate is in an elastic state, according to the Mises yield criterion, (23a) gives the limit for the possible maximum elastic residual strain ε_{01} for the plate bulk material. This is because first, the surface stress of a nanoelement depends on the applied electric potential [Haiss et al. 1998]; second, the deformation (hence the bending stiffness) can be controlled by adjusting the applied electric potential [Weissmüller et al. 2003; Kramer et al. 2004]; third, the maximum residual elastic strain (or the maximum residual elastic stress) is limited by the yield strength [Diao et al. 2006].

Equation (34) gives a linear scaling law for the normalized bending stiffness (D/D_0) of a nanoplate. Similar scaling has been previously observed in many physical properties at the nanoscale [Wang et al. 2006]. It shows that the thinner a nanoplate is, the larger its normalized bending stiffness will be. The first term of (34) is the relative effect of surface elasticity on the bending stiffness of a nanoplate. If the Poisson ratio of the surface is the same as that of the bulk material (that is, $\nu_2 = \nu_1$), this term is identical to Miller and Shenoy's analytical result for a nanoplate [Miller and Shenoy 2000]. The second term quantifies the relative effect of the initial surface stress on the bending stiffness of a nanoplate.

Equation (34) can be rewritten as

$$\frac{D-D_0}{D_0} = \frac{6S(1-\nu_1^2)}{(1-\nu_2^2)E_1 h} - \frac{\tau_0}{E_1 h} F(\nu_1),$$

where

$$F(\nu_1) = 2\nu_1(1+\nu_1). \tag{35}$$

For normal metallic nanoplates, the initial surface stress τ_0 is of the same order of the surface modulus S [Cammarata and Sieradzki 1994]. Atomistic simulations show that the surface modulus and the initial surface stress of a nanofilm can be either positive or negative [Miller and Shenoy 2000; Gurtin et al. 1976]. Equation (34) shows that an initial tensile surface stress tends to reduce the bending stiffness of a nanoplate.

Based on continuum elasticity, supplemented by surface elasticity [Miller and Shenoy 2000; Gurtin and Murdoch 1975] we have performed a number of numerical simulations on the pure bending of a nanoplate to validate the analytical predictions obtained in this paper. Firstly, we have numerically confirmed that when the initial surface stress is absent the analytical result of (34) (or Miller and Shenoy's

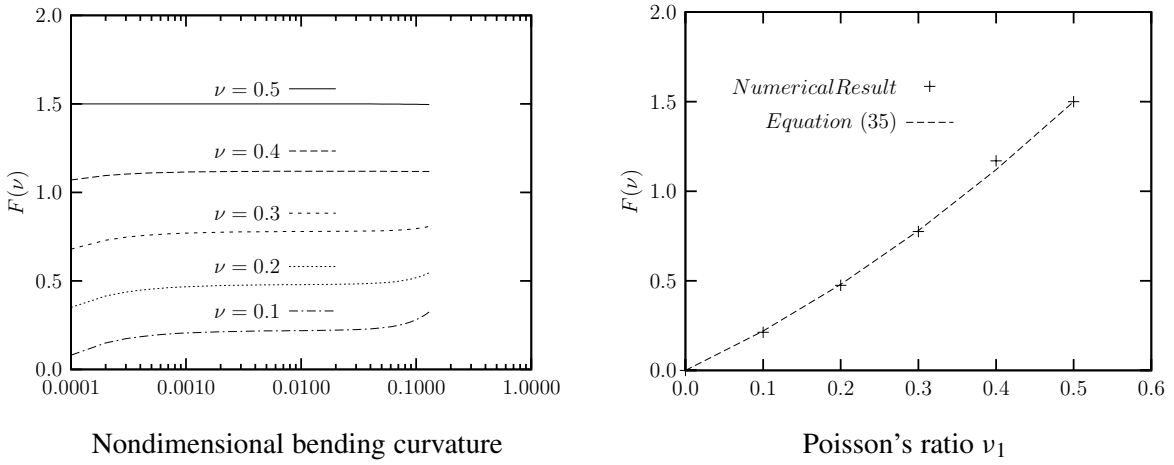

Figure 2. Comparison of the simplified analytical prediction with numerical simulations: F versus nondimensional bending curvature $1/R$ (left), and versus the Poisson's ratio ν_1 (right).

analytical result [Miller and Shenoy 2000]) provides exact predictions. Secondly, when the surface elasticity is ignored (that is, $S = 0$) and the Poisson ratio of the core material is fixed ($\nu_1 > 0$), the relative effect of the initial surface stress on the bending stiffness of a nanoplate is proportional to $\tau_0/(E_1 h)$, as predicted by (34). Thirdly, when the value of $\tau_0/(E_1 h)$ is fixed, the relative effect of the initial surface stress τ_0 on the bending stiffness of a nanoplate is a function of the Poisson ratio of the core material ν_1, as shown is in Figure 2. The left half of the figure shows that $F(\nu_1)$ is almost a constant over the normalized bending curvatures ranging from 0.0005 to 0.05 for a fixed value of ν_1 (the normalized bending curvature is h/R). We see on the right that the numerical result $F(\nu_1)$ is nearly identical to that of analytical prediction in (35). Although the analytical results obtained in this paper are derived from the small deformation theory, the numerical tests (Figure 2) provide us with sufficient confidence that the analytical results can be used in optimal design or experimental measurements for deformations up to a normalized bending curvature of 0.1 (that is, $h/R = 0.1$). Beyond this value of curvature, deviations occur as a result of the plate thickness reduction [Zhu 2007]. Note that the analytical results obtained in this section can be mathematically deduced from the analysis of the previous section (see Equation (20)) when the thickness t of the top and the bottom layers tends to zero. However, we have not been tempted by this limiting process as it would require us to relate the bulk elastic constant E to the surface modulus S, whereas there is no reason why such a relationship should exist.

For a nanobeam with a rectangular cross-section of thickness h and width b, as shown in Figure 3, left, the initial axial residual stress is $\sigma_0^x = -2\tau_0/h - 2\tau_0/b$, where τ_0 is the initial surface stress. When this nanobeam is bent by a pure moment, a plain stress deformation mode is created. Following the above analysis procedure, the total stress within the bulk material of the nanobeam in the axial direction can be calculated as

$$\Sigma^x(y) = \frac{E_1}{R} y - \frac{\nu_1 \tau_0}{R} - \frac{\nu_1 \sigma_0^x}{2R}(h - 2y) + \sigma_0^x \tag{36}$$

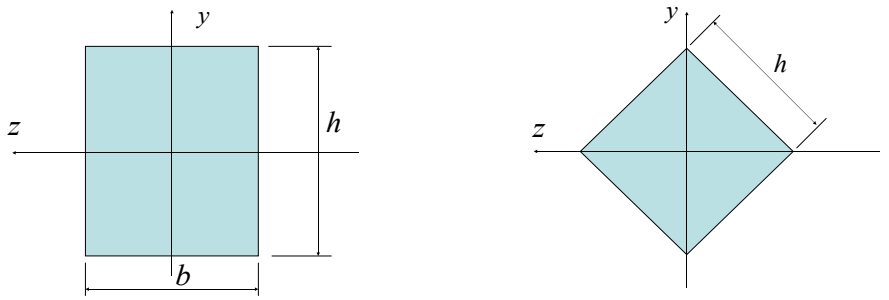

Figure 3. Left: a rectangular cross-section with the neutral axis z parallel to the sides. Right: a square cross-section with the neutral axis z coincided to the diagonal.

and the total surface stress in the x direction can be obtained as

$$\tau^x(y,z)=\begin{cases}\tau_0+Sh/(2R) & (y=h/2 \text{ and } 0<z<b),\\ \tau_0+\dfrac{Sy}{R}-\dfrac{\nu_1\tau_0 h}{2R}-\dfrac{\nu_1\tau_0}{R}y & (-h/2\le y\le h/2 \text{ and } z=0 \text{ or } b),\\ \tau_0-Sh/(2R) & (y=-h/2 \text{ and } 0<z<b),\end{cases} \tag{37}$$

where the Poisson ratio of the surface is assumed to be the same as that of the bulk material.

The elastic bending capacity is

$$\begin{aligned} M&=\frac{Sbh^2}{2R}+\int_{-h/2}^{h/2}2\left(\frac{S}{R}y-\frac{\nu_1\tau_0}{R}y\right)y\,dy+\int_{-h/2}^{h/2}\Sigma^x(y)\,by\,dy\\ &=\frac{Sbh^2}{2R}+\frac{Sh^3}{6R}-\frac{\nu_1\tau_0h^3}{6R}+\frac{E_1bh^3}{12R}+\frac{\nu_1\sigma_0^x}{12R}bh^3. \end{aligned} \tag{38}$$

Therefore the bending stiffness of the nanobeam is

$$D=M/(1/R)=\frac{Sbh^2}{2R}+\frac{Sh^3}{6R}-\frac{\nu_1\tau_0h^3}{6R}+\frac{E_1bh^3}{12}+\frac{\nu_1\sigma_0^x}{12}bh^3. \tag{39}$$

As the bending stiffness of the bulk beam is $D_0=E_1bh^3/12$, the relative effect of the initial surface stress and the surface elasticity is

$$\begin{aligned} \frac{D-D_0}{D_0}&=\frac{6S}{E_1h}+\frac{2S}{E_1b}+\frac{\nu_1\sigma_0^x}{E_1}-\frac{2\nu_1\tau_0}{E_1b}\\ &=\frac{6l_n}{h}+\frac{2l_n}{b}-\frac{4\nu_1\tau_0}{E_1b}-\frac{2\nu_1\tau_0}{E_1h}=\frac{6l_n}{h}+\frac{2l_n}{b}+\frac{(2h+b)\nu_1}{(b+h)(1-\nu_1)}\varepsilon_0^x, \end{aligned} \tag{40}$$

where, as before the internal length parameter $\ell_n=S/E_1$, and

$$\varepsilon_0^x=\frac{1}{E_1}(\sigma_0^x-\nu_1\sigma_0^y-\nu_1\sigma_0^z)=-\frac{2\tau_0}{E_1bh}(b+h)(1-\nu_1) \tag{41}$$

is the initial residual elastic strain in the bulk nanobeam in the x direction. According to the Mises yield criterion,

$$|\varepsilon_0^x| \le \frac{(b+h)(1-\nu_1)}{\sqrt{b^2+h^2-bh}}\varepsilon_y, \tag{42}$$

where ε_y is the uniaxial yield strain of the beam bulk material.

For a nanobeam with a square cross-section (that is, $b = h$), Equation (40) reduces to

$$\frac{D-D_0}{D_0} = \frac{8l_n}{h} - \frac{6\nu_1\tau_0}{E_1 h} = \frac{8l_n}{h} + \frac{3\nu_1}{2(1-\nu_1)}\varepsilon_0^x. \tag{43}$$

The first term in (43) is identical to Miller and Shenoy's analytical result (namely $(D - D_0)/D_0 = 8S/(Eh) = 8\ell_n/h$) for a nanobeam with a rectangular cross-section in the absence of the initial stress [Miller and Shenoy 2000]. Metallic nanomaterials can be used to make nanoactuators and the initial surface stress τ_0 can be controlled by the application of an electric potential [Haiss et al. 1998; Weissmüller et al. 2003; Kramer et al. 2004]. Equations (34) and (40) show that the effect of surface elasticity S on the bending stiffness of a nanoplate or nanobeam vanishes when its thickness h reaches about 100 nm, while the effect of the initial residual stress is proportional to ε_{01} which could be retained at a level up to a few percent by the application of an electric potential even for microplates and beams. Equations (34) and (40) provide a reliable estimate of the combined effects of surface elasticity S and initial surface stress τ_0 on the bending stiffness (and hence the dynamic characteristics) of nanoplates and nanobeams. It has important applications both in the optimal design of nanostructures and in the measurement of their characteristics.

For completeness, we will also give, without details, the effect of initial surface stress and surface elasticity on the stiffness, if a nanobeam with square section of side length h is bent about a diagonal plane as shown in Figure 3, right,

$$\frac{D-D_0}{D_0} = \frac{4\sqrt{2}l_n}{h} + \frac{\nu_1\sigma_0^x}{E_1} = \frac{4\sqrt{2}l_n}{h} + \frac{\nu_1}{(1-\nu_1)}\varepsilon_0^x. \tag{44}$$

In this case, the effect of the surface elasticity on the bending stiffness, given by the first term of (44), is smaller than that given by [Miller and Shenoy 2000].

For either a nanoplate/nanobeam or a macro symmetric trilayer plate/beam, we assume that its bending stiffness and natural frequency are respectively D_0 and ω_0 when the initial residual stress and the surface elasticity (for nanoplate/nanobeam) are absent; and D and ω when the initial residual stress and the surface elasticity (for nanoplate/nanobeam) are present. The combined effect of the initial residual stress and the surface elasticity for nanoplate/nanobeam on its natural frequency therefore scales as

$$\omega/\omega_0 = (D/D_0)^{1/2}. \tag{45}$$

Lagowski et al. [1975] found experimentally that the normal mode of vibration of thin crystals depends strongly on the surface preparation. They related this to the initial surface stress effect, which was treated as an external force. However, Gurtin et al. [1976] argued that the combination of the initial surface stress and the residual stress in the bulk material would cancel their individual effects. They attributed the dependence of the normal mode of vibration of thin crystals on surface preparation to surface elasticity. We have shown conclusively that the dynamic response depends both on the initial

residual stress in the surfaces and the bulk and on surface elasticity at the nanoscale. Wang and Feng [2007] have also considered the combined effects of surface elasticity and residual surface tension on the natural frequency of microbeams. However, as they did not take into account the effect of the residual stress in the bulk material, their result is suspect.

4. Conclusion

A simple closed-form analytical solution identifying the effect of initial residual stresses (or strains) on the bending stiffness of a symmetric trilayer structure or a nanoplate/nanobeam has been obtained. At the macro- and microscales, the relative effect is at the level of the initial elastic residual strain. If the structure is made of a hyperelastic material (such as a conducting polymer) and the initial elastic residual stress (or strain) is controllable, the relative effect of the initial stress (or strain) could reach a few percent. At the nanoscale, if the thickness of the nanoplate/nanobeam is around 10 nm or smaller, then the surface elasticity rather than the initial surface stress generally has a stronger relative effect on the bending stiffness. The surface elasticity effect however reduces with an increase in the plate/beam thickness, but the initial surface stress effect can be retained at a constant level of up to the limit of elastic strain if it can be controlled, for example by the application of an electrical potential.

References

[Alici et al. 2005] G. Alici, P. Metz, and G. M. Spinks, "A mathematical model to describe bending mechanics of polypyrrole (PPy) actuators", pp. 1029–1034 in *Proceedings of the 2005 IEEE/ASME International Conference on Advanced Intelligent Mechatronics* (Monterey, CA, 2005), IEEE, Piscataway, NJ, 2005.

[Bunch et al. 2007] J. S. Bunch, A. M. Van der Zande, S. S. Verbridge, I. W. Frank, D. M. Tanenbaum, J. M. Parpia, H. G. Craighead, and P. L. McEuen, "Electromechanical resonators from grapheme sheets", *Science* **315**:5811 (2007), 490–493.

[Cammarata and Sieradzki 1994] R. C. Cammarata and K. Sieradzki, "Surface and interface stresses", *Annu. Rev. Mater. Sci.* **24** (1994), 215–234.

[Chen et al. 2006] C. Q. Chen, Y. Shi, Y. S. Zhang, J. Zhu, and Y. J. Yan, "Size dependence of Young's modulus in ZnO nanowires", *Phys. Rev. Lett.* **96**:7 (2006), 075505.

[Cuenot et al. 2004] S. Cuenot, C. Frétigny, S. Demoustier-Champagne, and B. Nysten, "Surface tension effect on the mechanical properties of nanomaterials measured by atomic force microscopy", *Phys. Rev. B* **69**:16 (2004), 165410.

[Diao et al. 2006] J. Diao, K. Gall, M. L. Dunn, and J. A. Zimmerman, "Atomistic simulations of the yielding of gold nanowires", *Acta Mater.* **54**:3 (2006), 643–653.

[Dodin et al. 2001] M. Dodin, V. Tabard-Cossa, P. Grütter, and P. Williams, "Quantitative surface stress measurements using a microcantilever", *Appl. Phys. Lett.* **79**:4 (2001), 551–553.

[Donadon et al. 2002] M. V. Donadon, S. F. M. Almeida, and A. R. de Faria, "Stiffening effects on the natural frequencies of laminated plates with piezoelectric actuators", *Compos. B Eng.* **33**:5 (2002), 335–342.

[Duan et al. 2005a] H. L. Duan, J. Wang, Z. P. Huang, and B. L. Karihaloo, "Eshelby formalism for nano-inhomogeneities", *Proc. R. Soc. Lond. A* **461**:2062 (2005), 3335–3353.

[Duan et al. 2005b] H. L. Duan, J. Wang, Z. P. Huang, and B. L. Karihaloo, "Size-dependent effective elastic constants of solids containing nano-inhomogeneities with interface stress", *J. Mech. Phys. Solids* **53**:7 (2005), 1574–1596.

[Duan et al. 2006] H. L. Duan, J. Wang, B. L. Karihaloo, and Z. P. Huang, "Nanoporous materials can be made stiffer than non-porous counterparts by surface modification", *Acta Mater.* **54**:11 (2006), 2983–2990.

[Freund 2000] L. B. Freund, "Substrate curvature due to thin film mismatch strain in the nonlinear deformation range", *J. Mech. Phys. Solids* **48**:6–7 (2000), 1159–1174.

[Freund and Johnson 2001] L. B. Freund and H. T. Johnson, "Influence of strain on functional characteristics of nanoelectric devices", *J. Mech. Phys. Solids* **49**:9 (2001), 1925–1935.

[Gurtin and Murdoch 1975] M. E. Gurtin and A. I. Murdoch, "A continuum theory of elastic material surfaces", *Arch. Ration. Mech. An.* **57**:4 (1975), 291–313.

[Gurtin et al. 1976] M. E. Gurtin, X. Markenscoff, and R. N. Thurston, "Effect of surface stress on the natural frequency of thin crystals", *Appl. Phys. Lett.* **29**:9 (1976), 529–530.

[Haiss et al. 1998] W. Haiss, R. J. Nichols, J. K. Sass, and K. P. Charle, "Linear correlation between surface stress and surface charge in anion adsorption on Au(111)", *J. Electroanal. Chem.* **452**:2 (1998), 199–202.

[He et al. 2004] L. H. He, C. W. Lim, and B. S. Wu, "A continuum model for size-dependent deformation of elastic films of nano-scale thickness", *Int. J. Solids Struct.* **41**:3–4 (2004), 847–857.

[Huang and Zhang 2006] S. S. Huang and X. Zhang, "Extension of the Stoney formula for film-substrate systems with gradient stress for MEMS applications", *J. Micromech. Microeng.* **16**:2 (2006), 382–389.

[Huang and Zhang 2007] S. S. Huang and X. Zhang, "Gradient residual stress induced elastic deformation of multilayer MEMS structures", *Sens. Actuators A Phys.* **134**:1 (2007), 177–185.

[Hui et al. 2000] C. Y. Hui, H. D. Conway, and Y. Y. Lin, "A reexamination of residual stresses in thin films and of the validity of Stoney's estimate", *J. Electron. Packag.* (*ASME*) **122**:3 (2000), 267–273.

[Klein 2000] C. A. Klein, "How accurate are Stoney's equation and recent modifications", *J. Appl. Phys.* **88**:9 (2000), 5487–5489.

[Kramer et al. 2004] D. Kramer, R. N. Viswanath, and J. Weissmüller, "Surface-stress induced macroscopic bending of nanoporous gold cantilevers", *Nano Lett.* **4**:5 (2004), 793–796.

[Lagowski et al. 1975] J. Lagowski, H. C. Gatos, and E. S. Sproles, Jr., "Surface stress and the normal mode of vibration of thin crystals: GaAs", *Appl. Phys. Lett.* **26**:9 (1975), 493–495.

[Lim and He 2004] C. W. Lim and L. H. He, "Size-dependent nonlinear response of thin elastic films with nano-scale thickness", *Int. J. Mech. Sci.* **46**:11 (2004), 1715–1726.

[Lu et al. 2006] P. Lu, L. H. He, H. P. Lee, and C. Lu, "Thin plate theory including surface effects", *Int. J. Solids Struct.* **43**:16 (2006), 4631–4647.

[Malzbender 2004] J. Malzbender, "Mechanical and thermal stresses in multilayered materials", *J. Appl. Phys.* **95**:4 (2004), 1780–1782.

[Masmanidis et al. 2007] S. C. Masmanidis, R. B. Karabalin, I. De Vlaminck, G. Borghs, M. R. Freeman, and M. L. Roukes, "Multifunctional nanomechanical systems via tunably coupled piezoelectric actuation", *Science* **317**:5839 (2007), 780–783.

[Miller and Shenoy 2000] R. E. Miller and V. B. Shenoy, "Size-dependent elastic properties of nanosized structural elements", *Nanotechnology* **11**:3 (2000), 139–147.

[Nemat-Nasser 2002] S. Nemat-Nasser, "Micromechanics of actuation of ionic polymer-metal composites", *J. Appl. Phys.* **92**:5 (2002), 2899–2915.

[Stoney 1909] G. G. Stoney, "The tension of metallic films deposited by electrolysis", *Proc. R. Soc. Lond. A* **82** (1909), 172–175.

[Thompson and Clyne 2001] J. A. Thompson and T. W. Clyne, "The effect of heat treatment on the stiffness of zirconia top coats in plasma-sprayed TBCs", *Acta Mater.* **49**:9 (2001), 1565–1575.

[Wang and Feng 2007] G.-F. Wang and X.-Q. Feng, "Effects of surface elasticity and residual surface tension on the natural frequency of microbeams", *Appl. Phys. Lett.* **90**:23 (2007), 231904.

[Wang et al. 2006] J. Wang, H. L. Duan, Z. P. Huang, and B. L. Karihaloo, "A scaling law for properties of nano-structured materials", *Proc. R. Soc. Lond. A* **462**:2069 (2006), 1355–1363.

[Weissmüller et al. 2003] J. Weissmüller, R. N. Viswanath, D. Kramer, P. Zimmer, R. Würschum, and H. Gleiter, "Charge-induced reversible strain in a metal", *Science* **300**:5617 (2003), 312–315.

[Xu and Zhang 2003] W.-H. Xu and T.-Y. Zhang, "Mechanical characterization of trilayer thin films by the microbridge testing method", *Appl. Phys. Lett.* **83**:9 (2003), 1731–1733.

[Zhou and Huang 2004] L. G. Zhou and H. C. Huang, "Are surfaces elastically softer or stiffer?", *Appl. Phys. Lett.* **84**:11 (2004), 1940–1942.

[Zhu 2007] H. X. Zhu, "Large deformation pure bending of an elastic plastic power-law-hardening wide plate: analysis and application", *Int. J. Mech. Sci.* **49**:4 (2007), 500–514.

[Zhu 2008] H. X. Zhu, "The effects of surface and initial stresses on the bending stiffness of nanowires", *Nanotechnology* **19**:40 (2008), 405703.

[Zhu and Karihaloo 2008] H. X. Zhu and B. L. Karihaloo, "Size-dependent bending of thin metallic films", *Int. J. Plast.* **24**:6 (2008), 991–1007.

Received 1 Dec 2008. Revised 20 Dec 2008. Accepted 31 Dec 2008.

HANXING ZHU: zhuh3@cf.ac.uk
School of Engineering, Cardiff University, Cardiff CF24 3AA, United Kingdom

JIANXIANG WANG: jxwang@pku.edu.cn
LTCS and Department of Mechanics and Engineering Science, College of Engineering, Peking University, Beijing 100871, China

BHUSHAN KARIHALOO: KarihalooB@cf.ac.uk
School of Engineering, Cardiff University, Cardiff CF24 3AA, United Kingdom